Synthesis, structural characterization and NMR studies of group 10 metal complexes with macrocyclic amine *N*-heterocyclic carbene ligands

Taotao Lu,[a] *Zhiming Liu,*[b] *Carlos A. Steren,*[b] *Fan Fei,*[a] *Tabitha M. Cook,*[b] *Xue-Tai Chen*,*[a] *and Zi-Ling Xue*,*[b]

Abstract

A series of Ni(II), Pd(II) and Pt(II) complexes $[ML][PF_6]_2$ [L = L^1, M = Ni (**1**), Pd (**2**), Pt (**3**); L = L^2, M = Ni (**4**), Pd (**5**), Pt (**6**)] and $[Pt(L^2)(acac)]$ (**7**) have been prepared by the reactions of two tetradentate macrocyclic amine-NHC ligand precursors, $[H_2L^1][PF_6]_2$ and $[H_2L^2][PF_6]_2$, with $Ni(OAc)_2{\cdot}4H_2O$, $Pd(OAc)_2$ and $Pt(acac)_2$ in the presence of NaOAc. Complex **7** is isolated along with **6** from the same reaction between $[H_2L^2][PF_6]_2$ and $Pt(acac)_2$. There are two atropisomers in **1-3** and two achiral conformers in **4-6**. The crystal structures of **1-3** and one conformer of **4-6** (**4a-6a**) have been determined by single-crystal X-ray diffraction studies. The metal ion is found to reside in the cavity of the macrocyclic ring and adopts square-planar configuration. Detailed NMR studies including variable-temperature

[a] *State Key Laboratory of Coordination Chemistry, Nanjing National Laboratory of Microstructures, School of Chemistry and Chemical Engineering, Nanjing University, Nanjing 210023, China. E-mail: xtchen@nju.edu.cn; Fax: +86 25 89682309*

[b] Department of Chemistry, University of Tennessee, Knoxville, Tennessee 37996, USA. E-mail: xue@utk.edu†

Electronic supplementary information (ESI) available: Detailed crystallographic data,further figures of molecule structures, and 1D and 2D NMR spectra, powder XRD patterns, and X-ray structures of **6a** and **4a** in comparison with the solution structure of **4** from NMR.

NMR spectra reveal a dynamic interconverting process between two atropisomers of **1-3** in the solutions via a ring twisting mechanism. Two conformers in the equilibrated solution of **4-6**, probably arising from the orientation of two amine N-H bonds with respect to the coordination plane, exchange slowly. Time-dependent ^{1}H NMR spectra show that one conformer (**4a-6a**) in solution converts into the other (**4b-6b**) via the inversion of nitrogen atom.

Introduction

Since the isolation of the first stable N-Heterocyclic carbene (NHC) by Arduengo and co-workers in 1991,[1] NHCs and their metal complexes have garnered extensive research attention and witnessed widespread applications in catalysis,[2] advanced materials,[3] and medicines.[4] The electronic and steric effects of NHCs can be fine-tuned by modifying the heterocyclic moiety or the substituent on nitrogen atom.[5] Moreover, combination of NHC unit with other donor group would give versatile types of bidentate- or polydentate-functionalized NHC ligands with different geometric arrangements.[6] Recently, macrocyclic NHC-containing ligands,[6c] which contain at least one NHC donor group, have also been actively investigated since metal complexes with such macrocyclic NHC ligands have exhibited intriguing properties such as catalysis,[7] luminescence,[8] and antimicrobial activity.[9] Several types of macrocyclic NHC ligands have been reported, among which tetradentate macrocyclic NHC ligands are of particular interest because of their structural similarity to the classical macrocyclic ligands such as porphyrins. However, only few

tetradentate macrocyclic NHCs and their metal complexes are known. In 2001, Youngs et al. reported an Ag(I) complex with the first tetradentate marcocyclic NHC ligand containing two NHC units and two pyridine rings.[10] Subsequently, Ni(II) (**A**, Chart 1), Co(III), Fe(II) and Hg(II) complexes with this ligand have also been prepared.[11-14] Hahn et al. prepared a Pt(II) complex with a planar [16]ane-$P_2C^{NHC}_2$ (**B**, Chart 1) containing two phosphines and two NHC donors via a metal-template controlled synthetic procedure.[15] In addition to these metal complexes, Jenkins,[7a,16] Murphy,[17] Hahn,[18] Meyer,[19] Kühn[7b,20] and their co-workers have reported metal complexes with different types of tetradentate macrocyclic ligands constructed from four NHCs units with various linkers.

The coordination chemistry of saturated polyamine macrocyclic ligands has been well established and found many applications.[21] It is envisioned that combination of an NHC unit and a secondary amine would lead to interesting macrocyclic ligands. We have recently designed a novel hexadentate macrocyclic diamine-tetracabene ligand precursor, from which several Ag(I), Au(I), Ni(II) and Pd(II) complexes have been synthesized and structurally characterized.[22] We have also synthesized two tetradentate NHC-amine macrocyclic ligand precursors, $[H_2L^1][PF_6]_2$ and $[H_2L^2][PF_6]_2$ combining two benzimidazolium units with one secondary amine and one pyridine or two secondary amines (Chart 1), and their Ag(I) and Au(I) complexes.[23] In this work, we have synthesized a series of Ni(II), Pd(II), and Pt(II) complexes $[ML][PF_6]_2$ [L = L^1, M = Ni (**1**), Pd (**2**), Pt (**3**); L = L^2, M = Ni (**4**), Pd (**5**), Pt (**6**)] and [Pt(L^2)(acac)] (**7**) from the NHC precursors $[H_2L^1][PF_6]_2$ and $[H_2L^2][PF_6]_2$.

Extensive NMR studies including variable-temperature NMR spectra show a dynamic interconverting process between two atropisomers of **1-3** in solution via a ring twisting mechanism. Two achiral conformers probably arising from the orientation of two N-H bonds are found in the equilibrated solutions of **4**-**6**. The exchanges between **4a-6a** and their conformers **4b-6b** are slower than the NMR time scale. The crystal structures of **1**-**3** and one conformer **4**-**6** (**4a**-**6a)** have been determined. Their synthesis and structural features and detailed NMR studies of **1**-**7** are reported herein.

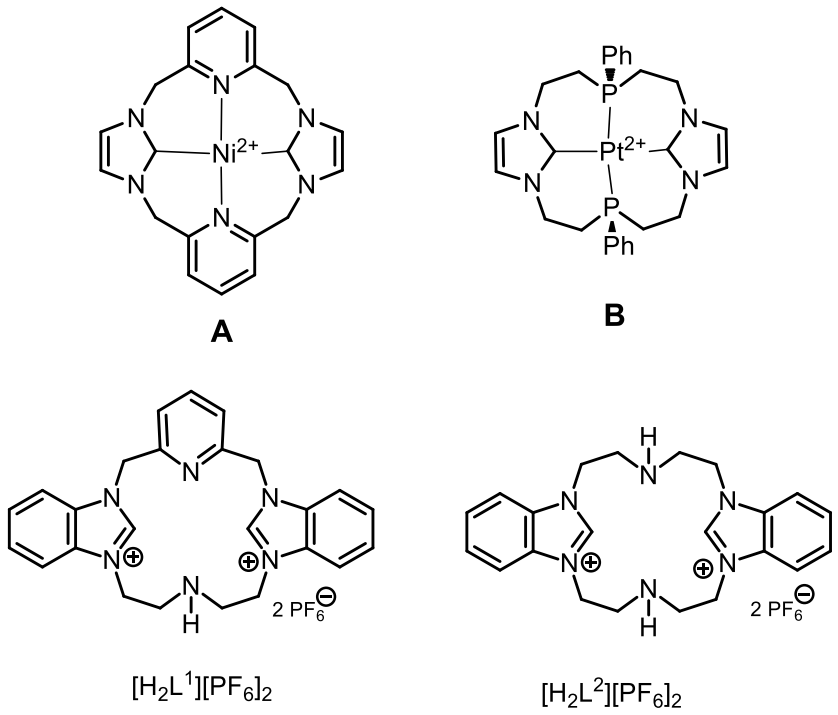

Chart 1 Selected examples of the reported metal complexes with tetradentate macrocyclic NHCs ligands and the ligand precursors $[H_2L^1][PF_6]_2$ and $[H_2L^2][PF_6]_2$ used in this study.

Results and discussion

Synthesis and characterization of complexes 1-7

Ni(II), Pd(II) and Pt(II) complexes with macrocyclic NHC ligands L^1 or L^2, $[ML][PF_6]_2$ [L = L^1, M = Ni (**1**), Pd (**2**), Pt (**3**); L = L^2, M = Ni (**4**), Pd (**5**), Pt (**6**)] and $[Pt(L^2)(acac)]$ (**7**), have been obtained by the reactions of $[H_2L^1][PF_6]_2$ and $[H_2L^2][PF_6]_2$[23] with $Ni(OAc)_2.4H_2O$, $Pd(OAc)_2$ or $Pt(acac)_2$ in the presence of NaOAc (Scheme 1). The amount of NaOAc is found to be essential for the isolation of the desired complexes. Pd(II) complexes **2** and **5** are prepared when 2.5 equiv of NaOAc is used. However, Ni(II) and Pt(II) analogues **1,3, 4** and **6** cannot be obtained with this amount of NaOAc. Instead, more NaOAc (using 10 equiv) is needed to successfully prepare them. It is noted that two Pt(II) complexes **6** and **7** with different molecular compositions are isolated from the same reaction between $Pt(acac)_2$, $[H_2L^2][PF_6]_2$ and NaOAc.

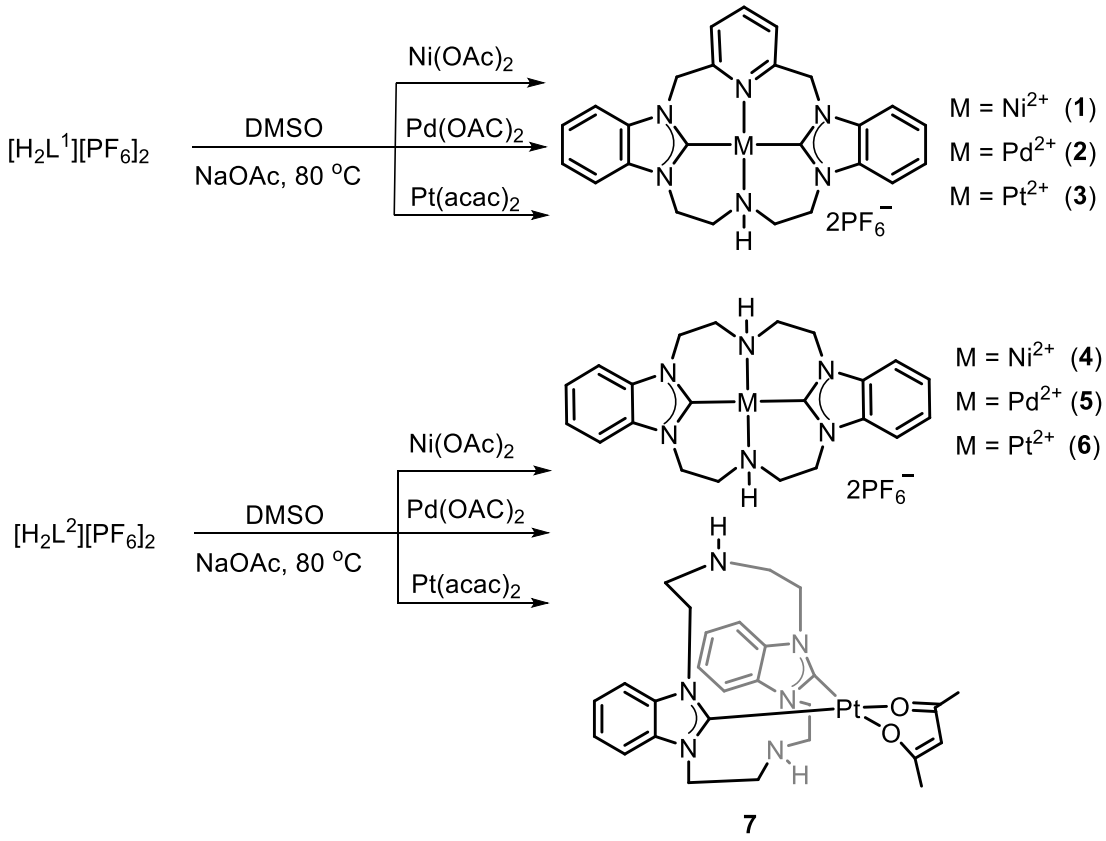

Scheme 1 Synthesis of Ni(II), Pd(II) and Pt(II) complexes **1**-**7**.

Complexes **1**-**7** are readily soluble in DMSO, DMF, CH_3CN and acetone. **7** is also soluble in CH_2Cl_2 and ether solvents. They have been characterized by elemental analysis, electrospray ionization mass spectrometry (ESI-MS), and NMR spectroscopy. In the mass spectroscopy of **1**-**6**, there are three peaks corresponding to $(M\text{-}2PF_6)^{2+}$, $(M\text{-}2PF_6\text{-}H)^{+}$and $(M\text{-}PF_6)^{+}$, respectively. Only one peak of *m/z* 668.33 is found for **7**. The ^1H NMR resonances detected at 9.55 and 9.56 ppm for *2H*-benzimidazolim protons of $[H_2L^1][PF_6]_2$ and $[H_2L^2][PF_6]_2$,[23] respectively, are not observed in the ^1H NMR spectra of **1**-**7**. Moreover, the ^{13}C NMR signals of carbene carbon atoms are found in the range of 153.4-173.1 ppm, showing a significant downfield shift in comparison with those of the NHC precursors (142.80 ppm for

$[H_2L^1][PF_6]_2$, 142.46 ppm for $[H_2L^2][PF_6]_2$).[23] The carbene carbon resonance in the range of 173.1-170.5 ppm found in **1-3** are significantly downfield shifted relative to those for **4-6** (163.2-160.3 ppm) and **7** (153.4 ppm). In the case of **7**, an acetylacetonate (acac) ligand is present to coordinate to Pt(II) ion, which is shown by two sharp ^{1}H NMR peaks at 5.64 ppm and 1.81 ppm with a 1:6 intensity ratio detected for C*H* and CH_3 groups, respectively. Three ^{13}C NMR resonances for the acac ligand are found at 185.4 (*C* = O), 101.9 (*C*H) and 26.1 (*C*H_3) ppm, respectively, which is consistent with the reported Pt(II)-acac complexes.[24] Detailed NMR data show that two atropisomers exist in **1-3** and two achiral conformers in the equilibrated solutions of **4-6** (as discussed in the next section).

Molecular structures of **1-3** and conformers **4a-6a** have been fully elucidated by single-crystal X-ray diffraction analyses (Tables S1-S2). Crystals of **1**·CH_3CN, **2** and **3** were obtained by slow evaporation of the acetonitrile from solutions of complexes **1-3**, while those of **4a-6a** were grown by vapor diffusion of ether into concentrated acetonitrile solutions of complexes **4-6**. **1**·CH_3CN crystallizes in the monoclinic space group *P*2/*c* while **2**, **3** and **4a-6a** crystallize in the triclinic space group *P*-1. Their structures are shown in Fig. 1 with selected structural parameters listed in Tables 1 and 2.

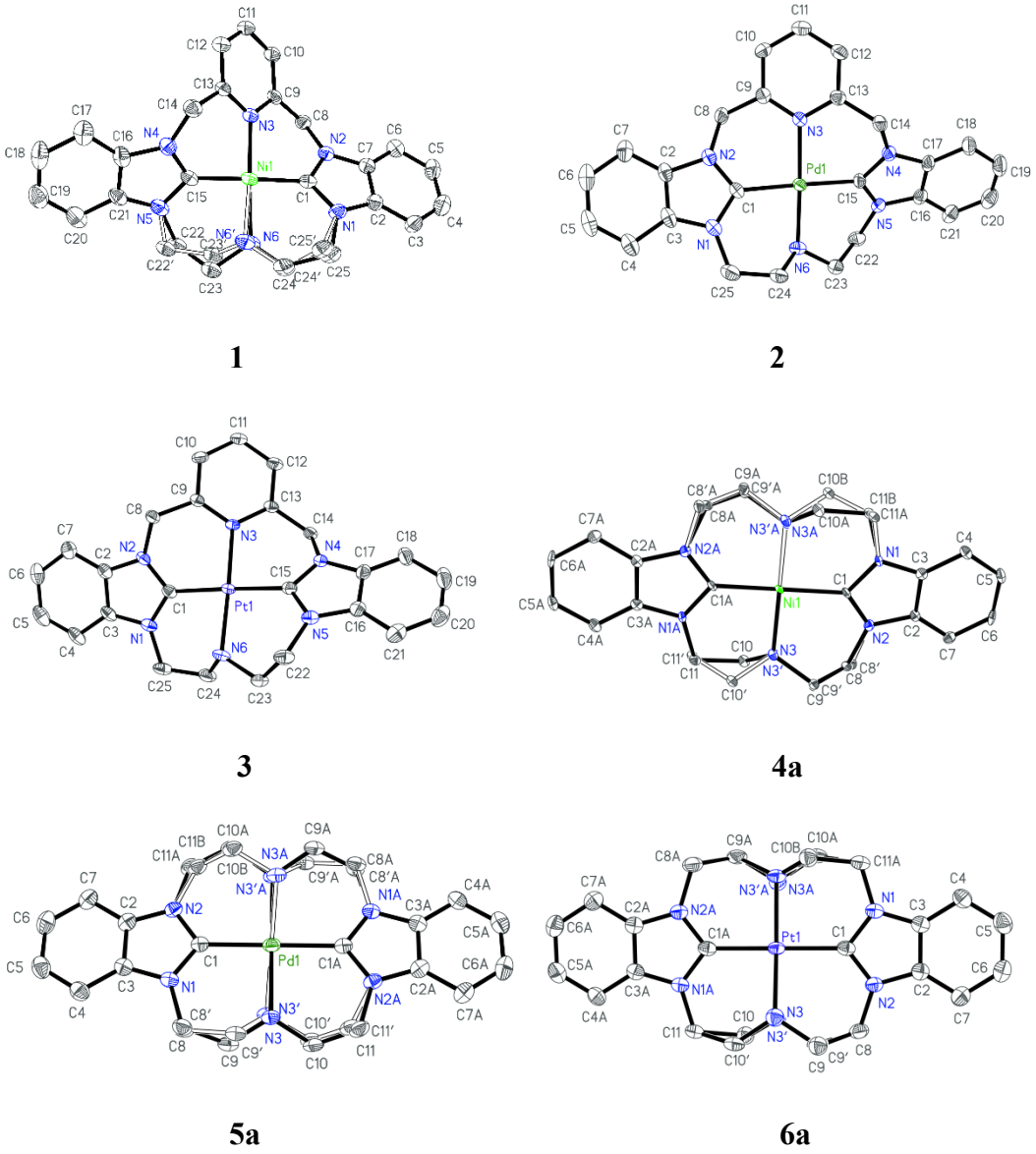

Fig. 1 Structures of **1**-**3** and **4a**-**6a**. Anions, solvent molecules, and hydrogen atoms including N-*H* are omitted for clarity. Ellipsoids are at 30% probability.

The crystals of **1**-**3** are comprised of two atropisomers, while there is only one conformer in the crystals of **4a**-**6a**. The central metal ion in **1**-**3** and **4a**-**6a** is found to reside in the cavity of the macrocyclic ring and adopts a slightly distorted square planar configuration. The coordination of two carbene carbon atoms and two nitrogen atoms give rise to the fusion of four six-membered chelate rings.

1-**3** exhibit a saddle-shaped conformation, in which the whole macrocyclic ligand is seriously twisted (Fig. S1). The pyridine ring is not in the central coordination plane defined by the metal ion and the four donors, giving a dihedral angle of 34.49° for **1**, 27.37° for **2** and 26.98° for **3**. Furthermore, the two benzimidazolylidene rings are also inclined relative to the coordination plane with dihedral angles of 33.12°/33.51° for **1**, 24.93°/27.36° for **2** and 25.38°/26.99° for **3**. Similar conformation is found in the Ni(II) complex with bisNHC-bispyridine macrocyclic ligand (**A**, Chart 1).[11] One ethylene linker along with the adjacent amine proton is located on one side of the coordination plane while the other ethylene linker is on the opposite side. The carbon atom attached to the amine in the former ethylene linker is nearly in the coordination plane.

The metal ion resides on a crystallorgraphic inversion center in complexes **4a**-**6a**. In contrast to the similar twisted conformation in **1**-**3**, **4a**-**6a** are distinctly different. **4a** also adopts a twisted structure, in which the two benzimidazolylidene planes are nonplanar with the central coordination plane with dihedral angles of 21.09°/21.11°, smaller than those (24.93°-33.51°) found for **1**-**3**. The two ethylene linkers on the two sides of amine group are located on the same side of the coordination plane in **4a**. In contrast, **5a**-**6a** are more planar than **4a**, indicating that the larger Pd(II) and Pt(II) ions fit the cavity of the larger L^2 ligand better than the Ni(II) ion. The two benzimidazolylidene planes are nearly co-planar with the coordination plane in **5a**-**6a** (0.04°/0.00°) (Fig. S2). The two ethylene linkers on the two sides of amine group have nearly identical conformations and the two carbon

atoms attached to the same amine are located in the same side of the coordination plane.

The Ni-C bond lengths of 1.875(6), 1.876(6) Å in **1** are shorter than those in **4a** (1.953(6) Å) but are comparable to those in macrocyclic Ni-C_{NHC} complexes.[8b,16a,16c,18b,20a] Similarly, Pd-C in **2** (2.002(5), 1.990(4) Å) and Pt-C in **3** (1.983(4), 1.997(4) Å) are also shorter than the corresponding metal-bonds in **5a** (2.050(3) Å) and **6a** (2.042(4) Å), respectively. The C-M-C and N-M-N bond angles in **1**-**3** are in the range of 174.1°-178.3°, while those of **4a**-**6a** are 180° due to the presence of the inversion centre. These suggest that the structures of **4a**-**6a** are in nearly ideal square planar geometry. In short, the bond lengths and angles in **1**-**3** and **4a**-**6a** closely match those reported in group 10 metal complexes with macrocyclic NHC ligands.[8b,16a,16c,17,18b,20a]

The amine nitrogen atom (N6) and the adjacent four carbon atoms (C22, C23, C24, C25) of the ethylene linker are disposed in two positions with the occupancy ratio of 1:1 in **1**. Similarly, the two symmetrically related amine N atoms and the adjacent four C atoms (C8, C9, C10, C11) are also disordered and located at site occupancies of 0.718 and 0.282 for **4a**, 0.827 and 0.173 for **5a**, 0.859 and 0.141 for **6a**.

Table 1 Selected bond lengths (Å) and angles (°) in **1**-**3** (major and minor components)[a]

	1	**2**	**3**
M-C1	1.875(6)	2.002(5)	1.983(4)
M-C15	1.876(6)	1.990(4)	1.997(4)
M-N3	1.955(5)	2.069(4)	2.060(3)
M-N6	1.98(2)	2.062(4)	2.063(3)
M-N6'	1.94(3)	---	---
C15-M-C1	178.3(2)	178.1(2)	178.08(12)
N6-M-N3	174.1(5)	178.12(16)	177.95(11)
C15-M-N6	92.5(4)	91.29(18)	86.46(14)
C15-M-N3	90.7(2)	90.59(17)	91.50(13)
C1-M-N6	85.8(4)	86.95(18)	91.62(14)
C1-M-N3	91.0(2)	91.17(17)	90.42(13)
C1-M-N6'	93.1(6)	---	---
C15-M-N6'	85.2(6)	---	---
N6'-M-N3	173.7(7)	---	---

[a] N6'-M and N6'-M-N3 are the minor components

Table 2 Selected bond lengths (Å) and angles (°) of **4a**-**6a** (major and minor components)[a]

	4a	**5a**	**6a**
M-C1	1.953(6)	2.050(3)	2.042(4)
M-N3	1.918(7)	2.119(3)	2.103(4)
M-N3'	2.119(19)	1.984(16)	2.05(3)
C1A-M-C1	180.0	180.0	180.0
N3A-M-N3	180.0	180.0	180.0
C1-M-N3A	92.3(3)	90.05(13)	89.69(16)
C1-M-N3	87.7(3)	89.95(13)	90.31(16)
N3'-M-C1	90.6(4)	86.6(4)	90.3(3)
N3A'-M-C1	89.4(4)	93.4(4)	89.7(3)

[a] N3'-M is the minor components

Two structural differences between **1**-**3** and **4a**-**6a** should be emphasized here: (a) Conformations of the macrocyclic rings are different. **1**-**3** adopts a twisted structure with the nonplanarity between the coordination plane, pyridine and benzimidazolylidene rings. **4a** also exhibits a twisted structure with the inclination of benzimidazolylidene rings relative to the coordination plane. But both **5a** and **6a** have more planar conformations in that the two benzimidazolylidene planes are nearly

co-planar with the coordination plane. (b) The two ethylene linkers on the two sides of the same amine group are each located on the opposite side of the coordination plane in **1**-**3** while those of **4a**-**6a** are located on the same side. Due to the presence of the N-H bonds, the two six-membered chelating rings attached to the same amine group give a C_1 symmetry for **1**-**3**. These different structural features could be related to the varied solution behaviours.

NMR studies and dynamic behaviours

It has been demonstrated that five- or six-membered chelating ring may exhibit ring twisting (ring inversion) processes in solution.[25] Similar dynamic processes have been observed in several group 10 metal complexes with tridentate pincer ligands, in which two six-membered chelate rings are fused together.[26-29] The two fused chelating rings would twist together to give an interconversion between two atropisomers. For example, variable-temperature (VT) NMR studies have revealed dynamic behaviour in Pd(II) complexes with tridentate NHC-containing ligands such as lutidine-bis(NHC) [27,28] and bis(ethylene)amine-bis(NHC).[29] In the lutidine-bis(NHC) Pd(II) complexes,[27a,27b] two C_2 symmetric atropisomers with a puckered conformation interconvert on the NMR timescale via the ring twisting process (equation 1, Scheme 2). Similar dynamic interconversion between two atropisomers occurs in the bis(ethylene)amine-bis(NHC) Pd(II) complexes (equation 2, Scheme 2).[29] However, the presence of the N−H renders the two ethylene linkers on the two sides of the NH group unequivalent, resulting in C_1 symmetry for the two

atropisomers.

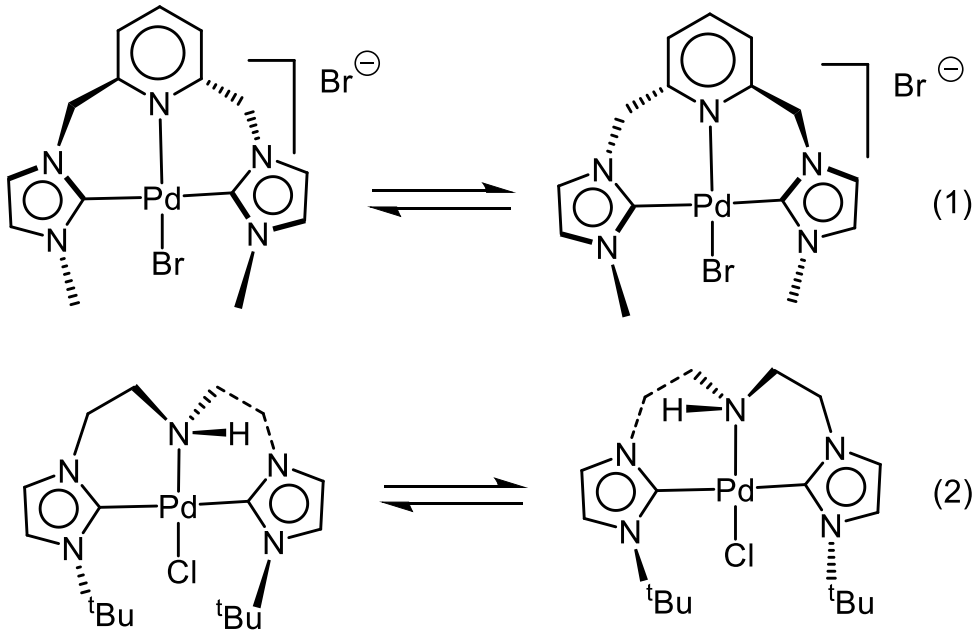

Scheme 2 The ring twisting process in lutidine-bis(NHC) and bis(ethylene)amine-bis(NHC) Pd(II) complexes.[27,29]

The metal complex with a tetradentate macrocyclic NHC-containing ligand such as the Ni(II) complex with a bispyridine-bisNHC ligand (**A**, Chart 1) can be regarded as the fusion of four six-membered chelating rings and is thus expected to exhibit the ring twisting process.[11] However, the VT NMR studies show that Ni(II) complex **A** remains static even at 80 °C.[11] Kühn et al. have revealed a dynamic ring twisting process for a Ni(II) complex with a macrocyclic 16-membered tetraNHC ligand,[20a] which was suggested to occur via a planar transition state.

Complexes **1**-**6** are the macrocyclic complexes constructed by the similar fragments as lutidine-bis(NHC) and bis(ethylene)amine-bis(NHC) Pd(II) complexes. It is thus interesting to probe whether a dynamic interconversion occurs in their

solutions. VT ^{1}H NMR spectra have been recorded for **1**-**7** in acetone-d_6, revealing fluxional behaviours in **1**-**3** at 185-295 K while the exchanges in **4**-**6** in solution at 295 K are not observed in ^{1}H NMR, suggesting they are slower than the NMR scale.

As discussed above, the two atropisomers of **1**-**3** adopt a twisted conformation. Similar to the bis(ethylene)amine-bis(NHC) Pd(II) complex,[29] the presence of the N−H bond and the location of the two ethylene linkers on the opposite side of the coordination plane in **1**-**3** renders two ethylene linkers not magnetically equivalent. This can be clearly observed from the crystal structures of **1**-**3**, where one six-membered ring twisting up and the other twisting down relative to the coordination plane and the amine proton is proximal to one ethylene linker, but distant from the other. The VT ^{1}H NMR spectra of **1** recorded in acetone-d_6 at 185-295 K is shown in Fig. S3 with selected spectra in Fig. 2. At 295 K, a broad peak at 5.28 ppm is assigned as the proton of the secondary amine group. The broad peak at 6.23 ppm is due to the diastereotopic methylene bridge between the pyridine and the benzimidazolylidene groups. The three signals at 3.2-5.1 ppm arise from the protons of the ethylene linkers between the secondary amine and the benzimidazolylidene groups. The peak at 4.62 ppm is broader than those at 4.94 and 3.55 ppm. With temperature decreasing, the signal at 6.23 ppm at 295 K broadens gradually, reaches decoalescence at 270 K, and finally evolves into two multiplets at 185 K. This could correspond to the expected ring twisting process between two atropisomers, exchanging the diastereotopic protons of the bridging methylene group in axial and equatorial positions. The ring twisting process in **1**, shown in Scheme 3 with the

labelling of the protons involved in the dynamic process, would render the two mutual exchanges between H^1 and H^4, H^2 and H^3. Since the amine proton is far away from the bridging methylene group between pyridine and benzimidazolylidene, the chemical shifts of H^1 is identical to H^3 and H^2 is identical to H^4. Therefore, the ring twisting process is identical to the exchange between H^1 and H^2. From the decoalescene temperature, $\Delta G^{\ddagger}_{270K}$ is estimated to be 12.6 kcal mol^{-1}.[20a] On decreasing the temperature from 295 to 185 K, the signals at 4.94 and 3.55 ppm become broader and develop into the multiplets. More interestingly, the signal at 4.62 ppm broadens, reaches the decoalescence at 270 K, and finally develop into two broad multiplets at 185 K. $\Delta G^{\ddagger}_{270K}$ is estimated to be 12.9 kcal mol^{-1} from the decoalescence temperature of 270 K.[20a] Both $\Delta G^{\ddagger}_{270K}$ values are nearly identical, consistent with the fact that both exchanges are due to the same dynamic process. From 265 K to 185 K, a broad peak at 2.67 ppm appears, which could be due to the ethylene linker that is broadened into the baseline or overlapped with the peak from the residual water at 295 K. The assignment of the signals (Fig. S16) are based on ^{13}C gHSQCAD and ^{13}C gCOSY spectra (Figs. S17-18) at 253 K in acetone-d_6. There are two sets of NMR signals for the ethylene linker due to the presence of the proton of the amine group. Similar assignments (Fig. S10) have been performed for 1D and 2D NMR spectra at 298 K (Figs. S11-15). It is interesting to note that the chemical shift of one proton (4.92 ppm) in one ethylene linker is significantly different from 2.67 ppm in the other at 253 K. Douthwaite et al. have found that chemical shifts of the resonances of the ethylene linker between imidazole and amine are in a wide range of 1.87 to 5.16 ppm

in the bis(ethylene)amine-bis(NHC) Pd(II) complexes.[29]

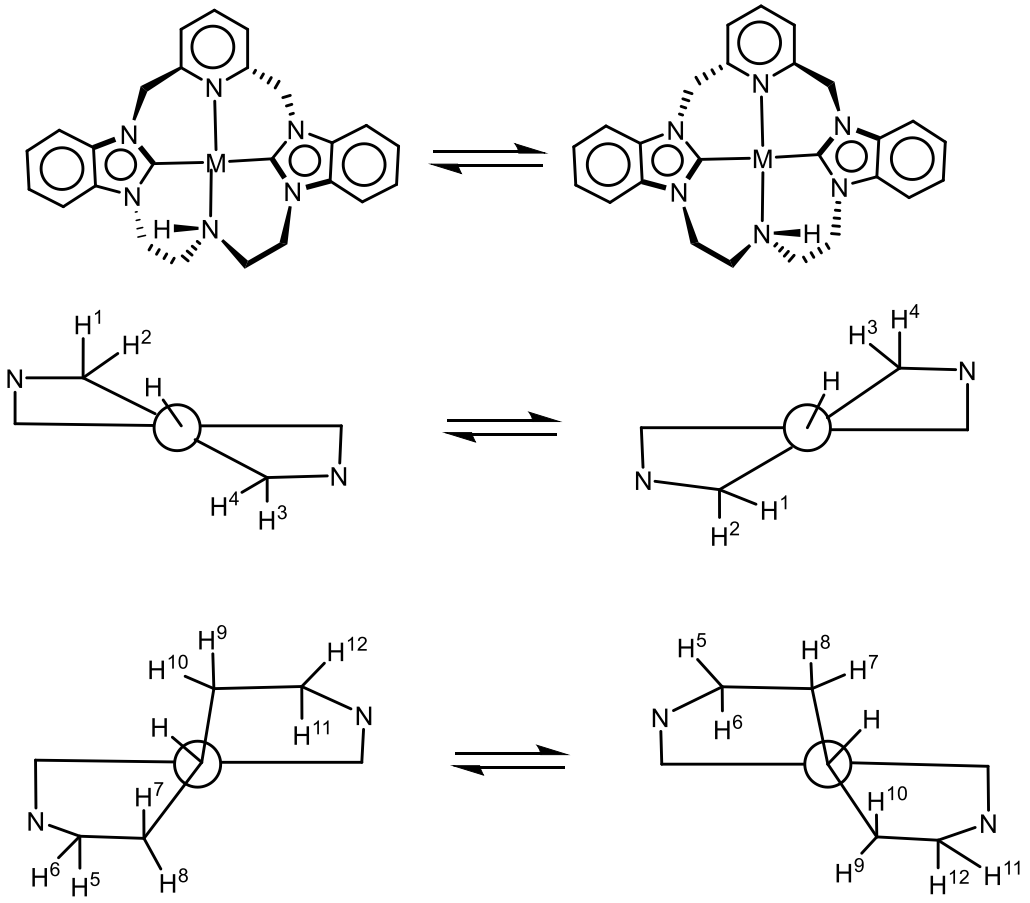

Scheme 3 Proposed ring twisting process between two atropisomers of **1**-**3** and the Newman projects of the lutidine-bis(NHC) metal and bis(ethylene)amine-bis(NHC) metal portions viewed along the amine-metal-pyridine bond, with the labelling of the protons involved in dynamic processes.

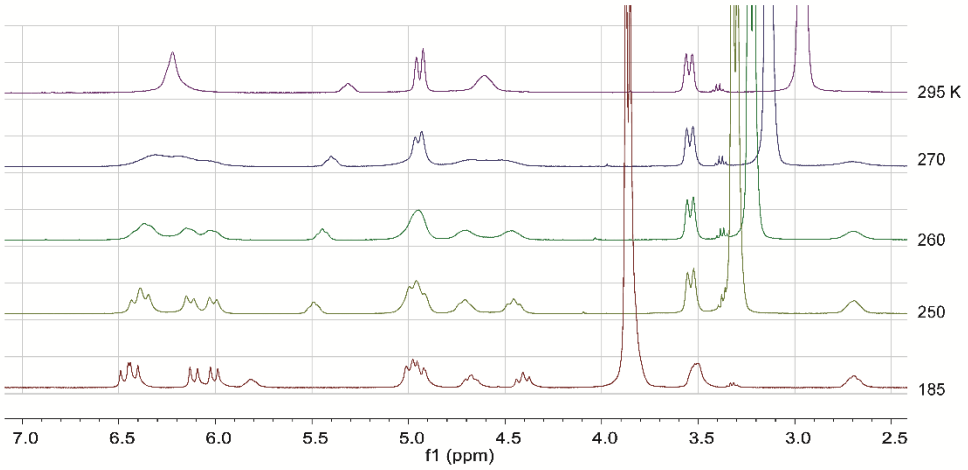

Fig. 2 Selected VT ^{1}H NMR spectra of **1** (from Fig. S4) in acetone-d_6.

The dynamic process would promote the four mutual exchanges between the eight protons of two ethylene linkers, *i.e.*, $H^5 \leftrightarrow H^{12}$, $H^6 \leftrightarrow H^{11}$, $H^7 \leftrightarrow H^{10}$, and $H^8 \leftrightarrow H^9$. The above assignments (Fig. S16) do not differentiate the two sets of the two ethylene linkers. The exchange of two signals at 3.51 ppm gives a temperature-independent signal, while the exchange between the peaks at 4.99 and 2.67 ppm would give an averaged signal expected at 3.88 ppm. It is noted that the expected signal at 3.88 ppm is not observed in 1D NMR spectrum due to the overlapping with the signals of water. By analogy, the signals at 4.70 and 4.45 ppm would exchange and average into a broad signal at 4.62 ppm observed at 295 K. The exchange of the signals at 4.92 and 4.90 ppm at 253 K give a slightly temperature-dependent signal at 4.94 ppm at 295 K. The temperature-dependent ^{1}H NMR signals (Figs. 2 and S4) are well explained by the mutual exchanges predicted by the ring twisting mechanism.

VT ^{1}H NMR spectra of **2** in acetone-d_6 are shown in Fig. S4 with selected spectra in Fig. 3. The peaks at 6.13 ppm for **2** at 295 K from the protons of the

methylene group between pyridine and benzimidazolylidene groups (H^1, H^2, H^3, H^4, Scheme 3) become very broad at 185 K. Compared with the temperature-dependent behaviours of the signals of the same methylene protons in **1**, the ring-twisting process in **2** is much faster than in **1**. Three signals at 3.0-5.5 ppm are observed for the protons from the ethylene linkers. The multiplet at 4.73 ppm at 295 K in **2** becomes gradually broader at 185 K, while the other two signals at 5.18 and 3.99 ppm are nearly temperature-independent. The assignments shown in Fig. S19 are made based on 1D and 2D NMR spectra at 298 K (Figs. S20-S25). Since the ring twisting process is much faster, the molecules of **2** are highly fluxional at 295 K. It is quite possible that these three ^{1}H NMR signals are due to the protons in the fast mutual exchanges, corresponding to an average structure. The signals at 5.18, 4.73 ppm are due to the exchange of four protons ($H^5 \leftrightarrow H^{12}$, $H^6 \leftrightarrow H^{11}$) adjacent to the benzimidazolylidene group while the signal at 3.99 ppm is due to the fast exchange of four protons (H_7, H_8, H_9, H_{10}) from the methylene groups attached to the amine group.

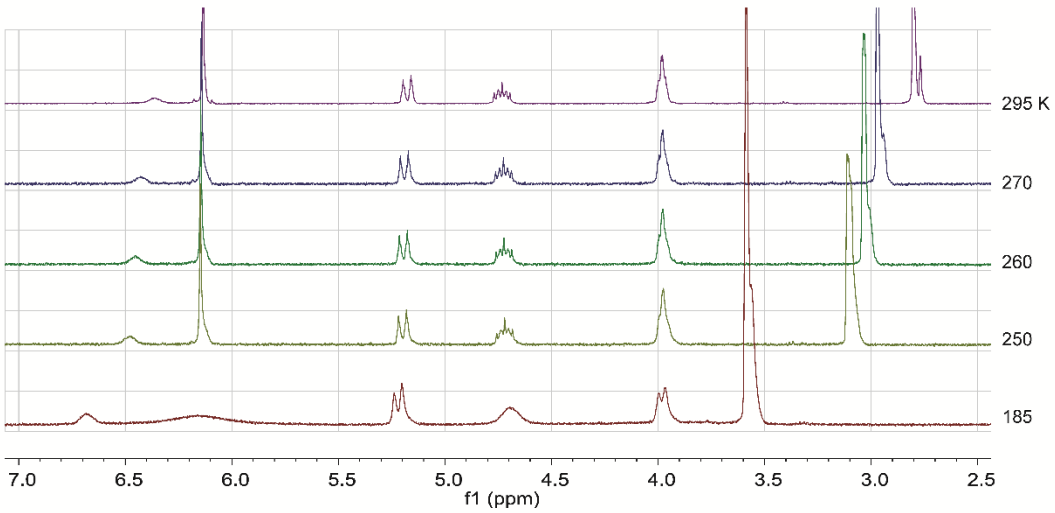

Fig. 3 Selected VT ^{1}H NMR spectra of **2** (from Fig. S5) in acetone-d_6.

In VT ^{1}H NMR spectra of **3** (Fig. S5 with selected spectra in Fig. 4), a signal at 6.07 ppm at 295 K from the two protons of the methylene bridge between pyridine and benzimidazolylidene groups broadens and develops into two broad signals at 185 K. Again, the ring twisting process in **3** is also much faster than in **1**. A signal at 5.16 ppm is nearly temperature-independent while the other three signals at 4.75, 4.15 and 4.01 ppm are getting broader at 185 K. The 1D and 2D NMR spectra were recorded at 298 K (Figs. S27-32). The assignments are shown in Fig. S26, which reveal that the four signals at 295 K are due to the four mutual exchanging protons. The two signals at 5.16, 4.75 ppm are due to the mutual exchanging protons of either $H^{6}\leftrightarrow H^{11}$ or $H^{5}\leftrightarrow H^{12}$. Similarly, the other two signals at 4.15 and 4.01 ppm are due to mutual exchanging protons of either $H^{7}\leftrightarrow H^{10}$ or $H^{8}\leftrightarrow H^{9}$. Since the signal at 5.16 ppm is nearly temperature-independent, it should result from the mutual exchanging protons with the close chemical shifts. (But we do not know which pair, $H^{6}\leftrightarrow H^{11}$ or $H^{5}\leftrightarrow H^{12}$.) The other three pairs of protons should have different chemical shifts. The ^{1}H NMR spectrum of **3** at 185 K shows that the molecules of **3** are still undergoing the dynamic process.

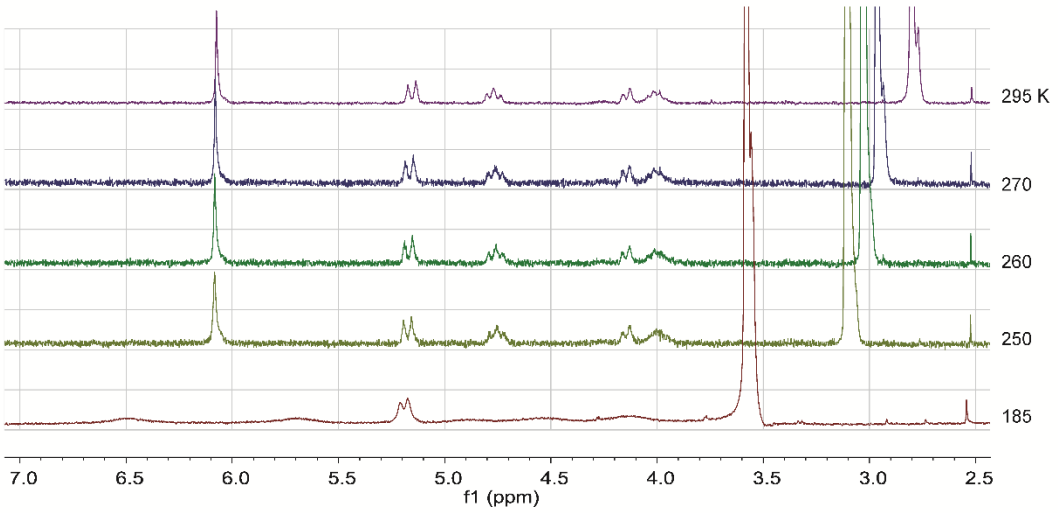

Fig. 4 Selected VT ^{1}H NMR spectra of **3** (from Fig. S6) in acetone-d_6.

VT ^{1}H NMR spectra recorded at 185-295 K for the equilibrated solutions of **4-6** in acetone-d_6 are shown in Figs. S6-S8, in which ^{1}H NMR signals appear to be temperature-independent, indicating that the exchanges in **4-6** are slow on the NMR time scale. In NMR spectra recorded at 293-403 K for the equilibrated solution of **4** in DMSO-d_6 (Fig. S6b), no exchange was observed either, indicating that even at 403 K, the exchange between **4a** and **4b** is slower than the NMR time scale. As discussed below, our NMR studies of solutions freshly prepared from crystals of **4a**-**6a** (Fig. S40 for **4a**, S47 for **5a**, and S54 for **6a**) show that **4a**-**6a** convert to conformers **4b**-**6b** slowly at room temperature, over a course of hours, eventually reaching equilibria.

A series of 2D NMR were recorded at 298 K in acetone-d_6. Their assignments are shown in Fig. S33 for **4**, Fig. S41 for **5** and Fig. S48 for **6**, which are based on the detailed 2D NMR spectra (Figs. S34-38 for **4**, Figs. S42-S46 for **5** and Figs. S49-S53 for **6**). These NMR data show that two conformers exist in the solutions of **4**-**6**, which are also consistent with the two ^{1}H NMR signals for amine protons in **4**-**6** and the

slightly different chemical shifts for the ethylene protons (Figs. S33, S41, S48). ^{1}H NMR selective decoupling experiments were carried out for **4** (Figs. S39A-D), revealing that the N-*H* signal of each conformer, a triplet, is coupled to the two equivalent H_A-C atoms (–CH_AH$_B$-N*H*-CH_AH$_B$-) on the two sides of the amine group, but is not coupled to the other two H_B atoms on the same C atoms.

The above assignments reveal that the four ethylene linkers are magnetically equivalent in both conformers of **4**-**6**. As described in the previous section on the crystal structures, the two ethylene linkers on the two sides of the same amine are similar in **5a** and **6a**, but quite different in **4a**. However, they are on the same side of the coordination plane in **4a**-**6a**. This structural feature would allow the two ethylene linkers to slightly adjust their positions in solution, resulting in a symmetric plane through the N---N axis for both conformers. NOESY and NMR experiments to determine $^{3}J_{H\text{-}H}$ coupling constants for solution of **4** show that the structure of **4** in solution adopts a more symmetric and planar structure, similar to the structure of **6a** in the solid state determined by the X-ray structure (Fig. S64). For example, torsion angles of **4** calculated from $^{3}J_{H\text{-}H}$ coupling constants are similar to those from the X-ray structure of **6a** but not **4a**. NOE (Nuclear Overhauser Effect) was observed for H atoms in **4** that are relatively close in space (ca. 2.4 Å) as in the crystal structure of **6a**. Crystal structure of **4a** shows that the distances among these H atoms are larger (2.7-2.8 Å) that unlikely show NOE.

In order to check if there are two conformers existing in our crystals, which were used for the X-ray single crystal diffractions and solution NMR studies, we have

picked-up several single crystals of **5a** and determined their crystal structures, which shows, that these crystals contain only **5a**. Furthermore, we have measured the X-ray powder diffraction patterns, which are each consistent with the calculated ones from the single crystal structural data (Figs. S61-63). This means that only one conformer **4a**-**6a** exists in our crystals.

We have then performed a time-dependent ^{1}H NMR studies for the freshly prepared solutions by dissolving the crystals of **4a**-**6a** at room temperature (Figs. S40, 47, 54). Here we take **5a** as an example, there are two ^{1}H NMR signals at 5.91 and 5.81 ppm observed for the amine protons. The signal of the latter grows with the elapse of time and the ratio of the two signals becomes constant after 4 h. These results indicate that conformer **5a** is transformed into **5b** to reach a chemical equilibrium in solution. From this, we can assign the set of NMR signals containing 5.91 ppm (N-*H*) for conformer **5a** (Fig. S41), whose structure has been determined by X-ray crystallography. The other set of NMR signals with the 5.81 ppm (N-*H*) peak shown in Fig. S41 are due to the other conformer **5b**. Similar assignment is made for **6a**-**6b** (Fig. S48). The sets of NMR signals containing 6.63 and 6.51 ppm (N-*H*) are due to conformers **6a** and **6b**, respectively. In the case of **4 (**Fig. S40), only one signal of one N-*H* proton is observed and the signal of the other N-*H* proton is overlapped with ethylene linkers. Considering that the signal of the N-*H* proton in both **5a** and **6a** is downfield shifted relative to those of **5b** and **6b**, we can assign the set of NMR signals with 4.64 and 4.59 ppm (N-*H*) to **4a** and **4b**, respectively (Fig. S33).

Although conformers **4a**-**6a** are assigned to those determined by X-ray

crystallography, the structures of the other conformers **4b**-**6b** are unknown yet. Considering the presence of two N-H bonds in **4**-**6**, it is reasoned that the orientation of two N-H bonds relative to the coordination plane would give two conformers for **4**-**6** as shown in Chart 2. In the conformer **4a**-**6a**, the two N-H bonds are located on each side of the coordination plane. The other conformer **4b**-**6b** could arise from the restricted inversion of one of the secondary amines in **4a**-**6a**. Such conformations arising from the orientation of N-H bonds have been demonstrated for the metal complexes with macrocyclic secondary amine ligands.[30] A more similar example has been found in the Ni(II) complex with the macrocyclic Schiff base Me_6[14]-4,11-dieneN_4 (Chart 3),[31] in which two conformers due to the orientation of the two N-H bonds, i.e., meso- and racemic-forms were found and interconvert in solution.[31a-31c] Furthermore the structures of both conformers were determined.[31d,31e] These reported examples indirectly supports our arguments about the structures of the conformers in **4**-**6**.

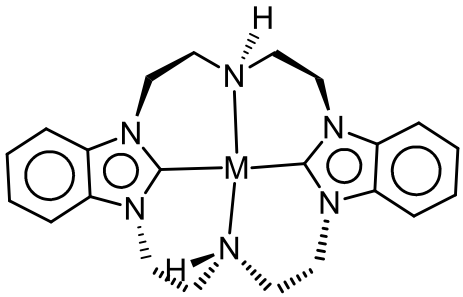

4a-6a

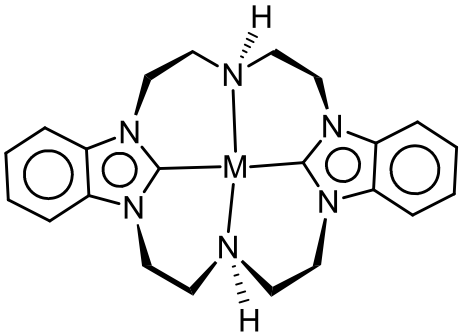

4b-6b

Chart 2 The two proposed conformers **4a**-**6a** and **4b**-**6b** arising from the orientation of N-H bonds relative to the macrocyclic ring.

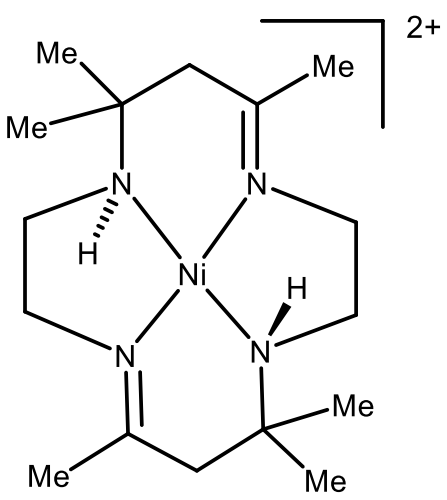

[Ni(*meso*-Me_6[14]diene)]$^{2+}$

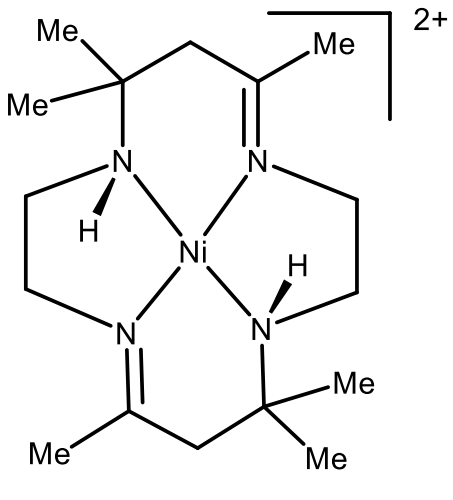

[Ni(*rac*-Me_6[14]diene)]$^{2+}$

Chart 3 Two conformers meso- and racemic-forms found in the Ni(II) complex with Me_6[14]-4,11-dieneN_4.[31]

The difference between **1**-**3** and **4**-**6** can be further outlined. It is noted that the two conformers arising from the orientation of the N-H bond is not possible in **1**-**3** due to the existence of only one N-H bond. However, two chiral conformers (atropisomers) exist in **1**-**3**, which are due to the restricted ring-twisting process and are interconverting on the NMR timescale as revealed by the VT NMR spectra. In contrast, the orientation of two N-H bonds give two conformers **4a**-**6a** and **4b**-**6b**, which are equilibrated in solution, but their interconversion are much slower and cannot be detected by VT-NMR spectroscopy. These differences could be ascribed to the varied conformations of the six-membered chelating rings. In **1**-**3**, the two atropisomers adopt the twisted structures with the two ethylene linkers attached to the same amine lying on the opposite side of the coordination plane. The presence of the N−H bond renders two ethylene linkers magnetically nonequivalent even though the

structures of **1-3** could relax to some extent in solution. In contrast, the two ethylene linkers on the two sides of the amine group are located on the same side of coordination plane, allowing them to easily relax into a more planar and symmetric structure even in the presence of one N-H bond. This could be the reasons why **4a-6a** do not undergo the ring twisting process. But the more restricted inversion of the one nitrogen atom in **4a-6a** gives rise to the other conformer **4b-6b**.

Finally, the molecule of **7** is found to be static in solution, as revealed by the VT ^{1}H NMR spectra of **7** (Fig. S9). The assignment of the NMR signals (Fig. S55) is based on the 1D and 2D NMR spectra at 298 K (Figs. S56-60).

Conclusions

In summary, two new macrocyclic amine-NHC ligand precursors $[H_2L^1][PF_6]_2$ and $[H_2L^2][PF_6]_2$ have been employed to prepare seven metal complexes **1-7** through reactions with $Ni(OAc)_2{\cdot}4H_2O$, $Pd(OAc)_2$ and $Pt(acac)_2$. The temperature-dependent NMR spectroscopic studies show that the two atropisomers in **1-3** are interconverting in solution via the ring twisting mechanism. There are two achiral conformers **4a-6a** and **4b-6b** probably arising from the orientation of the two N-H bonds in the equilibrated solutions. Exchanges between **4a-6a** and **4b-6b** are slow. Structural characterization shows that **1-3** and **4a-6a** adopt a slightly distorted square planar configuration but different conformation for the chelating rings. The slow exchanges of **4-6**, in contrast with **1-3**, could be due to the more planar structures of the full macrocyclic rings and the locations of the ethylene linkers on the same side of the

coordination plane.

Experimental

General procedures

All manipulations were performed under dry N_2, using standard Schlenk techniques unless otherwise stated. All other solvents and chemicals are commercial available and used as received without further purification. The ligand salts $[H_2L^1][PF_6]_2$ and $[H_2L^2][PF_6]_2$ were prepared according to the literature procedures.[23] Elemental analyses (C, H and N) were carried out on a Perkin-Elmer 240C analytic instrument. Mass spectra were measured with an ESI mass spectrometer (LCQ Fleet, Thermo Fisher Scientific). Powder X-ray diffraction (PXRD) data were recorded on a Bruker D8 ADVANCE X-ray powder diffractometer (Cu-Kα). NMR spectra for the ligand precursors were recorded on Bruker Avance 400 MHz spectrometer (^{1}H, 400 MHz; ^{13}C, 100 MHz) spectrometer at 295 K at Nanjing University (NJU). The other NMR measurements for **1-7** were performed at the University of Tennessee (UT). 1D and 2D NMR spectra of **1-7** at 295 K and **1** at 318 K were recorded on a Varian VNMRS 600 MHz spectrometer at UT equipped with an HCN cold probe. The NMR experiments at 253 K on **1** were performed on a Varian 500 MHz spectrometer equipped with an OneNMR probe at UT. VT NMR spectra were acquired on a Bruker Avance 400 MHz spectrometer equipped with a Broad Band Inverse (BBI) probe at UT.

Synthesis of $[Ni(L^1)][PF_6]_2$ (1)

To a solution of $[H_2L^1][PF_6]_2$ (200 mg, 0.286 mmol) in DMSO (5.0 mL) was added $Ni(OAc)_2 \cdot 4H_2O$ (78 mg, 0.314 mmol) and NaOAc (235 mg, 2.86 mmol). The reaction mixture was stirred at 80 °C for 12 h and then cooled to room temperature and filtered over celite. The filtrate was poured into water (50 mL) to precipitate a crude solid, which was filtered and washed with H_2O. The residue was then purified by recrystallization from CH_3CN/ether to afford **1** as a green solid (170 mg, 78.6% yield based on $[H_2L^1][PF_6]_2$). Anal. Calcd for $C_{25}H_{24}N_6NiP_2F_{12}$: C 39.66; H 3.20; N 11.10. Found: C 39.44; H 3.19; N 11.10%. ESI-MS: 233.17 $[M\text{-}2PF_6]^{2+}$, 466.44 $(M\text{-}2PF_6\text{-}H)^+$, 611.72 $[M\text{-}PF_6]^+$. ^1H NMR and ^{13}C NMR data (acetone-d_6, 500 MHz, 253 K): For the assignments, see Fig. S16.

Synthesis of $[Pd(L^1)][PF_6]_2$ (2)

To a solution of $[H_2L^1][PF_6]_2$ (200 mg, 0.286 mmol) in DMSO (5 mL) was added $Pd(OAc)_2$ (64 mg, 0.286 mmol) and NaOAc (60 mg, 0.715 mmol). The reaction mixture was stirred at 80 °C for 12 h. The mixture was cooled to room temperature and then filtered over celite. The filtrate was poured into water (50 mL) to precipitate a crude solid, which was filtered and washed with H_2O. The residue was dissolved in CH_3CN (2.0 mL) and then passed through a short alumina plug (pipette, 8.0 cm, washed with CH_3CN). The product was further purified by recrystallization from CH_3CN/ether to afford **2** as white solid (185 mg, 80.4% yield based on $[H_2L^1][PF_6]_2$). Anal. Calcd for $C_{25}H_{24}N_6PdP_2F_{12}$: C 37.31; H 3.01; N 10.44. Found: C

37.25; H 2.99; N 10.37%. ESI-MS: 257.08 $[M-2PF_6]^{2+}$, 513.17 $(M\text{-}2PF_6\text{-}H)^+$, 658.92 $[M-PF_6]^+$. ^1H NMR and ^{13}C NMR data (acetone-d_6, 400 MHz, 298 K): For the assignments, see Fig. S19.

Synthesis of $[Pt(L^1)][PF_6]_2$ (3)

To a solution of $[H_2L^1][PF_6]_2$ (200 mg, 0.286 mmol) in DMSO (5 mL) was added $Pt(acac)_2$ (112.3 mg, 0.286 mmol) and NaOAc (235 mg, 2.86 mmol). The reaction mixture was stirred at 80 °C for 48 h. The mixture was cooled to room temperature and then filtered over celite. The filtrate was poured into water (50 mL) to precipitate a crude solid, which was filtered and washed with H_2O and methanol. The residue was dissolved in acetone (2 mL) and then passed through a short alumina plug (pipette, 8 cm, washed with acetone:CH_2Cl_2 = 1:2) to give a crude product as a light yellow solid. The product was further purified by recrystallization from CH_3CN/ether to afford **3** as a white solid (96 mg, 37.4% yield based on $[H_2L^1][PF_6]_2$). Anal. Calcd for $C_{25}H_{24}N_6PtP_2F_{12}$: C 33.61; H 2.71; N 9.41. Found: C 33.52; H 2.55; N 9.65%. ESI-MS: 301.75 $[M-2PF_6]^{2+}$, 602.42 $(M\text{-}2PF_6\text{-}H)^+$, 748.00 $[M-PF_6]^+$. ^1H NMR and ^{13}C NMR data (acetone-d_6, 400 MHz, 298 K): For the assignments, see Fig. S26.

Synthesis of $[Ni(L^2)][PF_6]_2$ (4)

To a solution of $[H_2L^2][PF_6]_2$ (100 mg, 0.15 mmol) in DMSO (3.0 mL) was added $Ni(OAc)_2{\cdot}4\ H_2O$ (41 mg, 0.165 mmol) and NaOAc (123 mg, 1.50 mmol). The

reaction mixture was stirred at 80 °C for 12 h. The mixture was cooled to room temperature and then filtered over celite. The filtrate was poured into water (50 mL) to precipitate a crude solid, which was filtered and washed with H_2O. The residue was then purified by recrystallization from CH_3CN/ether to afford the product as brown solid (92 mg, 84.9% yield based on $[H_2L^2][PF_6]_2$). Anal. Calcd for $C_{22}H_{26}N_6NiP_2F_{12}$: C 36.54; H 3.62; N 11.62. Found: C 36.51; H 3.64; N 11.38%. ESI-MS: 216.17 $[M-2PF_6]^{2+}$, 431.25 $(M-2PF_6-H)^+$, 577.00 $[M-PF_6]^+$. ^1H NMR and ^{13}C NMR data (acetone-d_6, 400 MHz, 298 K): For the assignments of two conformers **4a** and **4b**, see Fig. S33.

Synthesis of $[Pd(L^2)][PF_6]_2$ (5)

To a solution of $[H_2L^2][PF_6]_2$ (300 mg, 0.45 mmol) in DMSO (6 mL) was added $Pd(OAc)_2$ (101 mg, 0.45 mmol) and NaOAc (92 mg, 1.13 mmol). The reaction mixture was stirred at 80 °C for 12 h. The mixture was cooled to room temperature and then filtered over celite. The filtrate was poured into water (50 mL) to precipitate a crude solid, which was filtered and washed with H_2O. The residue was dissolved in CH_3CN (2.0 mL) and then passed through a short alumina plug (pipette, 8 cm, washed with CH_3CN). The residue was then purified by recrystallization from CH_3CN/ether to afford the product as a light purple solid (240 mg, 69.2% yield $[H_2L^2][PF_6]_2$). Anal. Calcd for $C_{22}H_{26}N_6PdP_2F_{12}$: C 34.28; H 3.40; N 10.90. Found: C 34.36; H 3.63; N 10.93%. ESI-MS: 240.08 $[M-2PF_6]^{2+}$, 480.17 $(M-2PF_6-H)^+$, 625.92 $[M-PF_6]^+$. ^1H NMR and ^{13}C NMR data (acetone-d_6, 400 MHz, 298 K): For the assignments of two

conformers **5a** and **5b**, see Fig. S48.

Synthesis of $[Pt(L^2)][PF_6]_2$ (6) and $[Pt(L^2)(acac)]$ (7)

To a solution of $[H_2L^2][PF_6]_2$ (200 mg, 0.30 mmol) in DMSO (5.0 mL) was added $Pt(acac)_2$ (118 mg, 0.30 mmol) and NaOAc (246 mg, 3.0 mmol). The reaction mixture was stirred at 80 °C for 72 h. The mixture was cooled to room temperature and then filtered over celite. The filtrate was poured into water (50 mL) to give a crude solid, which was filtered and washed with H_2O. The residue was dissolved in acetone (2 mL) and then passed through a short alumina plug (pipette, 8 cm, washed with acetone(1/3-1)/dichloromethane(1) to give **7** (44 mg, 21.8% yield based on $[H_2L^2][PF_6]_2$) as a white solid and **6** as a brown solid (61 mg, 23.6% yield based on $[H_2L^2][PF_6]_2$).

6: Anal. Calcd for $C_{22}H_{26}N_6PtP_2F_{12}$: C 30.74; H 3.05; N 9.78. Found: C 30.83; H 3.34; N 9.86%. ESI-MS: 284.54 $[M-2PF_6]^{2+}$, 569.17 $(M-2PF_6-H)^+$, 714.56 $[M-PF_6]^+$. ^1H NMR and ^{13}C NMR data (acetone-d_6, 400 MHz, 298 K): For the assignments of two conformers **6a** and **6b**, see Fig. S41.

7: Anal. Calcd for $C_{27}H_{33}N_6O_2Pt$: C 48.50; H 4.97; N 12.57. Found: C 48.32; H 4.72; N 12.55%. ESI-MS: *m/z* 668.33[M−H]. ^1H NMR and ^{13}C NMR data (acetone-d_6, 400 MHz, 298 K): For the assignments, see Fig. S55.

X-ray structure determination

X-ray diffraction data were collected on a Bruker APEX DUO diffractometer

with a CCD area detector (Mo K_α radiation, λ = 0.71073 Å) at NJU.[32] The APEXII program was used to obtain frames of data and determining lattice parameters. SAINT was used to integrate the data. The absorption corrections were applied using SADABS.[33] The structures were solved by SHELXS-1997[34] and subsequently completed by Fourier recycling using SHELXS-1997 program.[35] All structures were solved using the direct method. The non-hydrogen atoms were refined by anisotropic displacement parameters. Crystallographic data, data collection, and refinement parameters for **1-6** are listed in Tables S1-S4 in ESI.

Conflicts of interest

There are no conflicts to declare.

Acknowledgments

We are grateful for the financial support from the Natural Science Grant of China (No. 21471078 to X.-T.C) and the U.S. National Science Foundation (CHE-1633870 to Z.-L.X).

References

1. A. J. Arduengo, R. L. Harlow, M. Kline, *J. Am. Chem. Soc.,* 1991, **113**, 361.
2. (a) J. A. Mata, M. Poyatos, E. Peris, *Coord. Chem. Rev.,* 2007, **251**, 841; (b) D. Pugh, A. A. Danopoulos, *Coord. Chem. Rev*., 2007, **251**, 610; (c) S. Díez-González, N. Marion, S. P. Nolan, *Chem. Rev*., 2009, **109**, 3612; (d) M.

Poyatos, J. A. Mata, E. Peris, *Chem. Rev*., 2009, **109**, 3677.

3. (a) R. Visbal, M. C. Gimeno, *Chem. Soc. Rev*., 2014, **43**, 3551; (b) L. Mercsa, M. Albrecht, *Chem. Soc. Rev.*, 2010, **39**, 1903; (c) N. Sinha, F. E. Hahn, *Acc. Chem. Res.*, 2017, **50**, 2167.
4. (a) A. Kascatan-Nebioglu, M. J. Panzner, C. A. Tessier, C. L. Cannon, W. J. Youngs, *Coord. Chem. Rev*., 2007, **251**, 884; (b) K. M. Hindi, M. J. Panzner, C. A. Tessier, C. L. Cannon, W. J. Youngs, *Chem. Rev*., 2009, **109**, 3859; (c) W. Liu, R. Gust, *Chem. Soc. Rev*., 2013, **42**, 755; (d) B. Bertrand, A. Citta, I. L. Franken, M. Picquet, A. Folda, V. Scalcon, M. P. Rigobello, P. Le Gendre, A. Casini, E. J. Bodio, *J. Biol. Inorg. Chem*., 2015, **20**, 1005.
5. (a) L. Cavallo, A. Correa, C. Costabile, H. Jacobsen, *J. Organomet. Chem.*, 2005, **690**, 5407; (b) S. Díez-González, S. P. Nolan, *Coord. Chem. Rev.*, 2007, **251**, 874.
6. (a) D. Pugh, A. A. Danopoulos, *Coord. Chem. Rev.*, 2007, **251**, 610; (b) M. Poyatos, J. A. Mata, E. Peris, *Chem. Rev*., 2009, **109**, 3677; (c) P. G. Edwards, F. E. Hahn, *Dalton Trans*., 2011, **40**, 10278; (d) O. Kühl, *Chem. Soc. Rev.*, 2007, **36**, 592; (e) H. M. Lee, C.-C. Lee, P.-Y. Cheng, *Curr. Org. Chem.*, 2007, **11**, 1491; (h) S. T. Liddle, I. S. Edworthy, P. L. Arnold, *Chem. Soc. Rev.*, 2007, **36**, 1732; (g) A. T. Normand, K. J. Cavell, *Eur. J. Inorg. Chem.*, 2008, **18**, 2781; (h) A. John, P. Ghosh, *Dalton Trans.,* 2010, **39**, 7183; (i) M. Bierenstiel, E. D. Cross, C*oord. Chem. Rev.*, 2010, **255**, 574; (j) C. Fliedel, P. Braunstein, *J. Organomet. Chem.,* 2014,**751**, 286; (k) F. E. Hahn, M. C. Jahnke, *Angew. Chem. Int. Ed*., 2008, **47**, 3122.

7. (a) S. A. Cramer, D. M. Jenkins, *J. Am. Chem. Soc.*, 2011, **133**, 19342; (b) J. W. Kück, M. R. Anneser, B. Hofmann, A. Pöthig, M. Cokoja, F. E. Kühn, *ChemSusChem*, 2015, **8**, 4056.
8. (a) P. J. Barnard, L. E. Wedlock, M. V. Baker, S. J. Berners-Price, D. A. Joyce, B. W. Skelton, J. H. Steer, *Angew. Chem. Int. Ed*., 2006, **45**, 5966; (b) N. J. Findlay, S. R. Park, F. Schoenebeck, E. Cahard, S. Zhou, L. E. A. Berlouis, M. D. Spicer, T. Tuttle, J. A. Murphy, *J. Am. Chem. Soc*., 2010, **132**, 15462; (c) N. Sinha, L. Stegemann, T. T. Y. Tan, N. L. Doltsinis, C. A. Strassert, F. E. Hahn, *Angew. Chem. Int. Ed*., 2017, **56**, 2785.
9. A. Melaiye, Z. Sun, K. Hindi, A. Milsted, D. Ely, D. H. Reneker, C. A. Tessier, W. J. Youngs, *J. Am. Chem. Soc*., 2005, **127**, 2285.
10. J. C. Garrison, R. S. Simons, J. M. Talley, C. Wesdemiotis, C. A. Tessier, W. J. Young, *Organometallics*, 2001, **20**, 1276.
11. M. V. Baker, B. W. Skelton, A. H. White, C. C. Williams, *Organometallics*, 2002, **21**, 2674.
12. K. Kawano, K. Yamauchi, K. Sakai, *Chem. Commun*., 2014, **50**, 9872.
13. I. Klawitter, M. R. Anneser, S. Dechert, S. Meyer, S. Demeshko, S. Haslinger, A. Pöthig, F. E. Kühn, F. Meyer, *Organometallics*, 2015, **34**, 2819.
14. M. V. Baker, D. H. Brown, R. A. Haque, P. V. Simpson, B. W. Skelton, A. H. White, C. C. Williams, *Organometallics,* 2009, **28**, 3793.
15. A. Flores-Figueroa, T. Pape, K. Feldmann, F. E. Hahn. *Chem. Commun*., 2010, **46**, 324.

16. (a) H. M. Bass, S. A. Cramer, A. S. McCullough, K. J. Bernstein, C. R. Murdock, D. M. Jenkins, *Organometallics,* 2013, **32**, 2160; (b) H. M. Bass, S. A. Cramer, J. L. Price, D. M. Jenkins, *Organometallics*, 2010, **29**, 3235; (c) Z. Lu, S. A. Cramer, D. M. Jenkins, *Chem. Sci*., 2012, **3**, 3081.

17. R. McKie, J. A. Murphy, S. R. Park, M. D. Spicer, S. Zhou, *Angew. Chem. Int. Ed*., 2007, **46**, 6525.

18. (a) F. E. Hahn, C. Radloff, T. Pape, A. Hepp, *Chem. Eur. J*., 2008, **14**, 10900; (b) C. Schulte to Brinke, F. E Hahn, *Dalton Trans*., 2015, **44**, 14315; (c) O. Kaufhold, A. Stasch, T. Pape, A. Hepp, P. G. Edwards, P. D. Newman, F. E. Hahn, *J. Am. Chem. Soc.*, 2009, **131**, 306; (d) F. E. Hahn, V. Langenhahn, T. Lügger, T. Pape, D. Le Van, *Angew. Chem. Int. Ed*., 2005, **44**, 3759.

19. S. Meyer, I. Klawitter, S. Demeshko, E. Bill, F. Meyer, *Angew. Chem. Int. Ed.*, 2013, **52**, 901.

20. (a) P. J. Altmann, D. T. Weiss, C. Jandl, F. E. Kühn, *Chem. Asian J.*, 2016, **11**, 1597; (b) M. R. Anneser, S. Haslinger, A. Pöthig, M. Cokoja, V. D'Elia, M. P. Högerl, J.-M. Basset, F. E. Kühn, *Dalton Trans.*, 2016, **45**, 6449; (c) M. R. Anneser, S. Haslinger, A. Pöthig, M. Cokoja, J.-M. Basset, F. E. Kühn, *Inorg. Chem.*, 2015, **54**, 3797.

21. (a) P. Chaudhuri, K. Wieghardt, *Prog. Inorg. Chem.*, 1987, **35**, 329; (b) H. Elias, *Coord. Chem. Rev.,* 1999, **187**, 37.

22. T. Lu, C.-F. Yang, L.-Y. Zhang, F. Fei, X.-T. Chen, Z.-L. Xue, *Inorg. Chem.*, 2017, **56**, 11917.

23. T. Lu, C.-F. Yang, F. Fei, X.-T. Chen, Z.-L. Xue, submitted to NJC

24. Y. Unger, D. Meyer, O. Molt, C. Schildknecht, I. Münster, G. Wagenblast, T. Strassner, *Angew. Chem. Int. Ed*., 2010, **49**, 10214.

25. (a) J. K. Beattie, *Acc. Chem. Res.*, 1971, **4**, 253; (b) C. J. Hawkins, R. M. Peachey, C. L. Szoredi, *Aust. J. Chem*., 1978, **31**, 973; (c) Y. Kuroda, M. Goto, T. Sakai, *Bull. Chem. Soc. Jpn.*, 1989, **62**, 3437.

26. (a) E. Díez-Barra, J. Guerra, I. López-Solera, S. Merino, J. Rodríguez-López, P. Sánchez-Verdú, J. Tejeda, *Organometallics*, 2003, **22***,* 541; (b) H. M. Lee, J. Y. Zeng, C. H. Hu, M. T. Lee, *Inorg. Chem.*, 2004, **43**, 6822.

27. (a) S. Gründemann, M. Albrecht, J. A. Loch, J. W. Faller, R. H. Crabtree, *Organometallics*, 2001, **20***,* 5485; (b) J. R. Miecznikowski, S. Gründemann, M. Albrecht, C. Mégret, E. Clot, J. W. Faller, O. Eisenstein, R. H. Crabtree*, Dalton Trans.*, 2003, 831. (c) F. E. Hahn, M. C. Jahnke, V. Gomez-Benitez, D. Morales-Morales, T. Pape, *Organometallics*, 2005, **24**, 6458; (d) F. E. Hahn, M. C. Jahnke, T. Pape, *Organometallics*, 2007, **26**, 150.

28. (a) N. Watarai, H. Kawasaki, I. Azumaya, R. Yamasaki, S. Saito, *Heterocycles*, 2009, **79**, 531; (b) R. E. Andrew, A. B. Chaplin, *Dalton Trans.*, 2014, **43**, 1413.

29. (a) R. E. Douthwaite, J. Houghton, B. M. Kariuki, *Chem. Commun*, 2004, 698; (b) J. Houghton, G. Dyson, R. E. Douthwaite, A. C. Whitwood, B. M. Kariuki, *Dalton Trans.*, 2007, 3065.

30. (a) B. Bosnich, C. K. Poon, M. L. Tobe, *Inorg. Chem.*, 1965, **4**, 1102; (b) R. Clay, J. Murray-Rust, P. Murry-Rust, *J. Chem. Soc., Dalton Trans.*, 1979, 1135; (c) L. G.

Warner, D. H. Busch, *J. Am. Chem. Soc.*, 1969, **91**, 4092.

31. (a) N. F. Curtis, Y. M. Curtis, H. K. J. Powell, *J. Chem. Soc. (A)*, 1966, 1015. (b) L. G. Warner, N. J. Rose, D. H. Busch, *J. Am. Chem. Soc.*, 1968, **90**, 6938; (c) A. M. Tait, D. H. Busch, *Inorg. Synth.*, 1978, **18**, 2; (d) M. F. Bailey, I. E. Maxwell, *Chem. Commun.*, 1966, 908; (e) S. Hajela, W. P. Schaeffer, J. E. Bercaw, *Acta Cryst. C*., 1992, **48**, 1767.
32. *SMART & SAINT Software Reference Manuals, version 6.45;* Bruker Analytical X-ray Systems, Inc.: Madison, WI, 2003.
33. G. M. Sheldrick, *SADABS: Software for Empirical Absorption Correction, version 2.05;* University of Göttingen: Göttingen, Germany, 2002.
34. G. M. Sheldrick, *SHELXS-1997, Program for Crystal Structure Solution*, University of Göttingen, Göttingen, Germany, 2008.
35. G. M. Sheldrick, *SHELXL-2014: Program for Crystal Structure Refinement;* University of Göttingen: Göttingen, Germany, 2014.